Desalination and Water Treatment
www.deswater.com

doi: 10.5004/dwt.2022.28519

261 (2022) 214–223
June

Surface ion-imprinted silica clay for adsorption of chromium(III) ions from aqueous with high selectivity

Junwen Li[a,†], He Li[a,†], Qiao-e Wang[b], Haiming Cheng[a,c,*]

[a]*Key Laboratory of Leather Chemistry and Engineering of Ministry of Education, Sichuan University, Chengdu 610065, China, emails: chenghaiming@scu.edu.cn (H. Cheng), 1206409276@qq.com (J. Li), 1562068778@qq.com (H. Li)*
[b]*Key Laboratory of Cosmetic, China National Light Industry, Beijing Technology and Business University, Beijing 100048, China, email: wangqe@th.btbu.edu.cn*
[c]*National Engineering Research Center of Clean Technology in Leather Industry, Sichuan University, Chengdu 610065, China*

Received 2 December 2021; Accepted 19 April 2022

ABSTRACT

A novel adsorbent ion-imprinted polymer–silica clay (IIP@SC) was prepared via surface ion imprinting technology by using silica clay (SC) as the support matrix and methacrylic acid as the ionic imprinting monomer. The adsorbent was characterized by Fourier-transform infrared spectroscopy, scanning electron microscopy, transmission electron microscopy, and X-ray diffraction. The prepared IIP@SC was applied for recovery of Cr(III) ions from aqueous solution. The selectivity properties of IIP@SC are evaluated. The results showed that the maximum adsorption capacity reached 157.98 mg/g in 30 min when the initial concentration of metal ions was 100 mg/L at pH 6.0. Adsorption kinetic and adsorption equilibrium studies demonstrated that the experimental data fitted well with the pseudo-second-order model and the Langmuir isotherm model. Competitive adsorption study showed that the prepared IIP@SC exhibits an efficient selectivity for Cr(III) ions.The prepared IIP@SC adsorbent can be a promising adsorbents for Cr(III) recovery from aqueous solutions with high selectivity.

Keywords: Chromium(III) ion; Ion-imprinted technology; Silica clay; Selective adsorption

1. Introduction

Heavy metal ions pollution in wastewater with is one of the most serious environment issues in modern society. The toxic metal ions can be enriched by organisms along the food chain, accumulate in human body and lead to chronic poisoning [1,2]. Chromium ions pollution are widely occurred in mining, electroplating, metal finishing, leather tanning, coatings and pigments [3–5]. Tanning process is an essential process to convert animal hides and skins into leather and to impart the leather with its unique characteristics. Chrome tanning agents are world widely used in tanning process so far [5–7]. However, only 70%–80% of chromium(III) (Cr(III)) tanning agents are fixed with the hide proteins in the traditional chrome tanning process, the effluent discharged after chrome tanning are of a huge concentration of Cr(III) ions [6,7]. Therefore the removal of Cr(III) ions from industrial wastewater is of great concern. Methods developed for removal of heavy metal ions from wastewater include ion exchange, biological operation, chemical precipitation, sedimentation, and adsorption [8–12]. Among them, adsorption is an effective method to remove Cr(III) ions due to its easy operation, low cost, good reusability, and excellent recovery efficiency. In order to solve the Cr(III) ions pollution in industrial wastewater, the development of Cr(III) adsorbents with high adsorption capacity and excellent selectivity is still important.

* Corresponding author.
† Both the authors contributed equally to this work.

Surface ion-imprinting technology has been applied as an effective way for solving the pollutions of heavy metal ions [13–15]. Many porous materials are commonly used as the support matrix, on which the imprinting polymer layer can be formed. The surface ion imprinted adsorbents not only can realize selectivity separation of heavy metal ions from wastewater, but also solves the innate limitations of traditional ion-imprinted polymer (IIP) such as heterogeneous distribution of the binding sites, incomplete template removal, and slow mass transfer for the target ions [16,17]. Therefore the surface structure of support matrix plays an important role in the adsorption capacity of IIP. Mesoporous materials have been paid attention a lot in recent years due to their unique characteristics such as adjustable pore size, large specific surface area, and high thermal stability [18–20].

Silica clay (SC) is a kind of mesoporous material consists of SiO_2, Al_2O_3 and Fe_2O_3 [21]. It is found that SC has unique properties including high porosity, large specific surface area, low economic cost and easy modification. Herein, SC was used as the carrier, on which carboxyl groups was ion imprinted to prepare IIP@SC for recovery of Cr(III) ions from aqueous. The adsorption study focused on the effect of operation parameters and the adsorption processes with various competing metal ions.

2. Materials and method

2.1. Materials

SC, chromic nitrate ($Cr(NO_3)_3$), and methyl methacrylate (MAA) were purchased from Kelong Chemicals (Chengdu, China). Ethylene glycol dimethacrylate (EGDMA) and 2,2′-azobisisobutyronitrile (AIBN) were purchased from Aladdin (Shanghai, China). Chromium(III) standard solution at 1.000 g/L was purchased from National Analysis and Testing Center (Beijing, China). All other reagents were analytical grade and used as received without further purification. The stock solution of Cr(III) (1,000 mg/L) was prepared by dissolving appropriate amount of $Cr(NO_3)_3$ in deionized water (18.2 MΩ).

2.2. Synthesis of IIP@SC

The surface ion imprinting onto SC was synthesized through radical-induced polymerization in combination with in-situ co-precipitation method. Briefly, 1.0 mmol of $Cr(NO_3)_3$ and 8.0 mmol of MAA were dissolved in 45 mL of methanol/acetonitrile (2:1,v/v) in a 150 mL of flask by stirring at room temperature for 30 min to form the complex of Cr(III)-MAA. Then, 2.0 g of SC, 4.0 mL of EGDMA and 0.1 g AIBN were added into the flask and the mixture was stirred at 70°C for 24 h in N_2 atmosphere to form Cr(III) ion-imprinted polymers onto SC (Cr(III)-IIP@SC). After that the mixture was filtered out and washed thoroughly with ethanol. 4.0 mol/L of HNO_3 was used for eluting the imprinted Cr(III) ions. Then the solids were desiccated at 65°C to constant weight and designed as IIP@SC. As a control, a non-imprinted adsorbent was prepared in the same way mentioned above but without the addition of Cr(III) ions and designed as NIP@SC. The synthesis process is illustrated in Fig. 1.

2.3. Characterization

Fourier-transform infrared spectroscopy (FT-IR) were recorded by a Nicolet iS10 FT-IR spectrometer (Thermo Fisher Scientific, USA) by KBr pellet method in the range

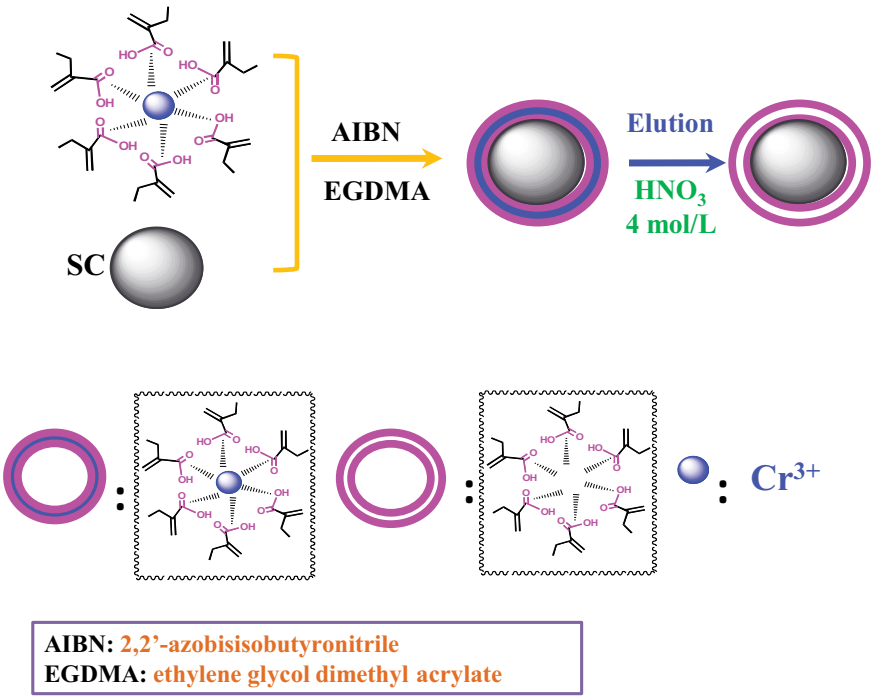

Fig. 1. Schematic of the synthesis procedures of Cr(III)-IIP@SC.

of 4,000~400 cm^{-1} with 2 cm^{-1} of resolution. Surface morphology was observed with a JSM 7500F scanning electron microscopy (SEM) (JEOL, Japan) and a FEI Tecnai G2 F20 S-TWIN transmission electron microscopy (TEM) (FEI, USA). The elemental compositions of the samples were measured by an INCA X-Max50 energy-dispersive X-ray spectroscopy (Oxford Instruments, UK). Crystal structure were characterized by an Empyrean X-ray diffraction analyzer (XRD) (Panax, Netherlands), using Cu Kα as the ray source (λ = 1.54059 Å), and the scanning range was 5°–90°. The zeta potential of the samples was detected by a Zetasizer Nano ZSP (Malvern, UK), and the pH of the suspension (1.0 mg/mL) was adjusted with sodium hydroxide or hydrochloric acid solution.

2.4. Batch adsorption experiments

The batch experiments of IIP@SC adsorption of Cr(III) ions were investigated in a serious of 50 mL polyethylene tubes. Briefly, certain amount (5–80 mg) of the prepared adsorbent and 30 mL solution of varying concentration of Cr(III) ions (20–600 mg/L) were added into the tube. The pH (2.0–6.0) of Cr(III) ion solutions, the contact time (5–200 min), at 25°C were investigated. The pH of the solution was adjusted to a desired value by 0.1 mol/L of HCl or NaOH. The concentration of Cr(III) ions before and after adsorption was measured by a 2,300 DV inductively coupled plasma–optical emission spectrometry (ICP-OES) (PerkinElmer, USA). All the adsorption experiments were performed three times. The adsorption capacity q_e (mg/g) and the percentage adsorption efficiency (R%) were calculated by Eqs. (1) and (2):

$$q_e = \frac{(C_0 - C_e) \times V}{m} \tag{1}$$

$$R = \frac{C_0 - C_e}{C_0} \times 100 \tag{2}$$

where C_0 (mg/L) and C_e (mg/L) are the initial and equilibrium concentrations of the metal ions, respectively; V (L) is the volume of the testing solution and m (g) is the weight of adsorbent.

2.5. Competing adsorption

To evaluate the adsorption selectivity of IIP@SC to Cr(III) ions with coexisting ions, competitive adsorptions of Cr(III)/Cr(VI) and Cr(III)/Pb(II) were investigated, respectively. 30 mg of the adsorbent with 30 mL of the solution containing 100 mg/L of each kind of metal ions was stirred at pH 6.0 and 25°C for 120 min. After adsorption, the concentration of metal ions before and after adsorption was determined by ICP-OES. The distribution ratio (K_d, L/g), selectivity coefficient K and the relative selectivity coefficient K' were calculated by Eqs. (3)–(5) [22]:

$$K_d = \frac{(C_0 - C_e)}{C_e} \times \frac{V}{m} \tag{3}$$

$$K_{\mathrm{Cr(III)}/M} = \frac{K_{d(\mathrm{Cr(III)})}}{K_{d(M)}} \tag{4}$$

$$K' = \frac{K_{\mathrm{Cr(III)-IIP-SC}}}{K_{\mathrm{NIP-SC}}} \tag{5}$$

Herein, the concentration of Cr(VI) ions in Cr(III)/Cr(VI) solution was determined using a diphenylcarbazide spectrophotometry assay [23].

3. Results and discussion

3.1. Characteristic

The FT-IR spectrum of SC showed peaks at 3,424; 1,630; 1,011 and 792 cm^{-1}, among which, 3,424 and 1,630 cm^{-1} are the stretching vibration and the bending vibration of hydroxyl group, while 1,011 and 792 cm^{-1} are the stretching vibration of Si–O–Si [24] (Fig. 2A). In comparison with the SC, the appearance of peaks at 2,972; 1,735; 1,386; 1,465

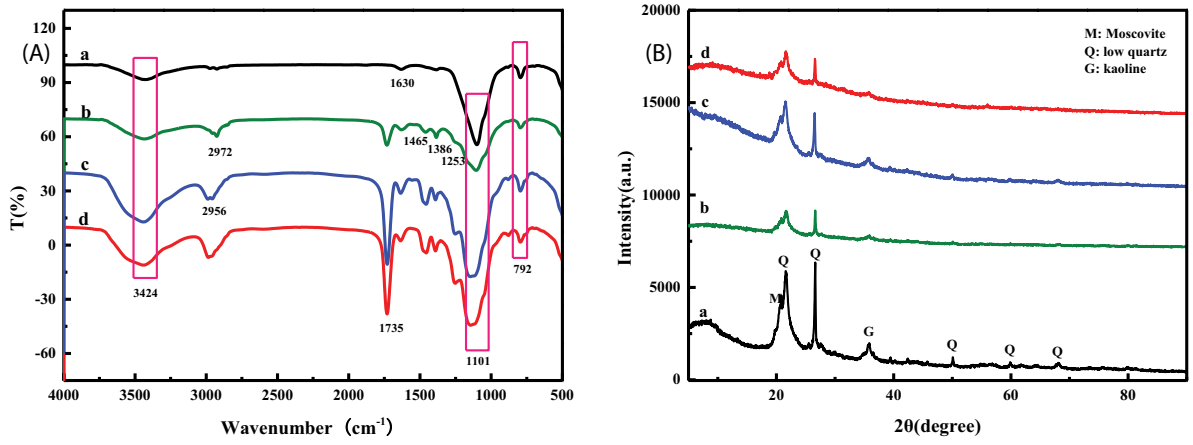

Fig. 2. (A) FT-IR spectra. a: SC; b: Cr(III)-IIP@SC; c: IIP@SC; d: NIP@SC and (B) XRD spectra. a: SC; b: Cr(III)-IIP@SC; c: IIP@SC; d: NIP@SC.

and 1,253 cm^{-1} indicated the formation of imprinted clay. Among them, the peak at 2,972 cm^{-1} could be assigned to C-H stretching vibration, while 1,386 and 1,465 cm^{-1} could be assigned to C–H bending vibration, the peak at 1,735 cm^{-1} is the stretching vibration of C=O and the peak at 1,253 cm^{-1} is assigned to the symmetrical stretching vibration of C–O–C, which belong to EGDMA and MAA [25]. The results illustrate that IIP@SC has been successfully prepared.

The XRD profiles of SC, Cr(III)-IIP@SC, IIP@SC and NIP@SC are shown in Fig. 2B. Silica clays are mainly composed of kaolinite, low temperature quartz (α-SiO_2) and Muscovite [26,27]. The formed ion-imprinted polymers are coated onto the surface, which did not change the crystal structure of SC but lead the reduction of intensity of sharp characteristic diffraction peak ranging from 15° to 40° (Fig. 2B).

Fig. 3 shows the SEM images of SC, IIP@SC and NIP@SC. It can be observed that SC is mainly composed of granular low-temperature quartz and tabular kaolin (Fig. 3e), which is consistent with the previous report [28]. After imprinting polymerization, the surface morphology of IIP@SC maintains porous structure (Fig. 3a) and the ion-imprinted layers formed on SC could be observed on the TEM images (Fig. S1). The particles of IIP@SC and NIP@SC show irregular and multi-deformed, and the size of IIP@SC (45–58 nm) are more uniform than that of NIP@SC (60–96 nm) (Fig. 3b and d).

The energy-dispersive X-ray spectroscopy analysis shows the composition of IIP@SC before and after elution of Cr(III) ions. The elemental composition of Cr in Cr(III)-IIP@SC is 1.30% (Fig. 4a), indicating that chromium ions has been successfully bound with the imprinted polymer.

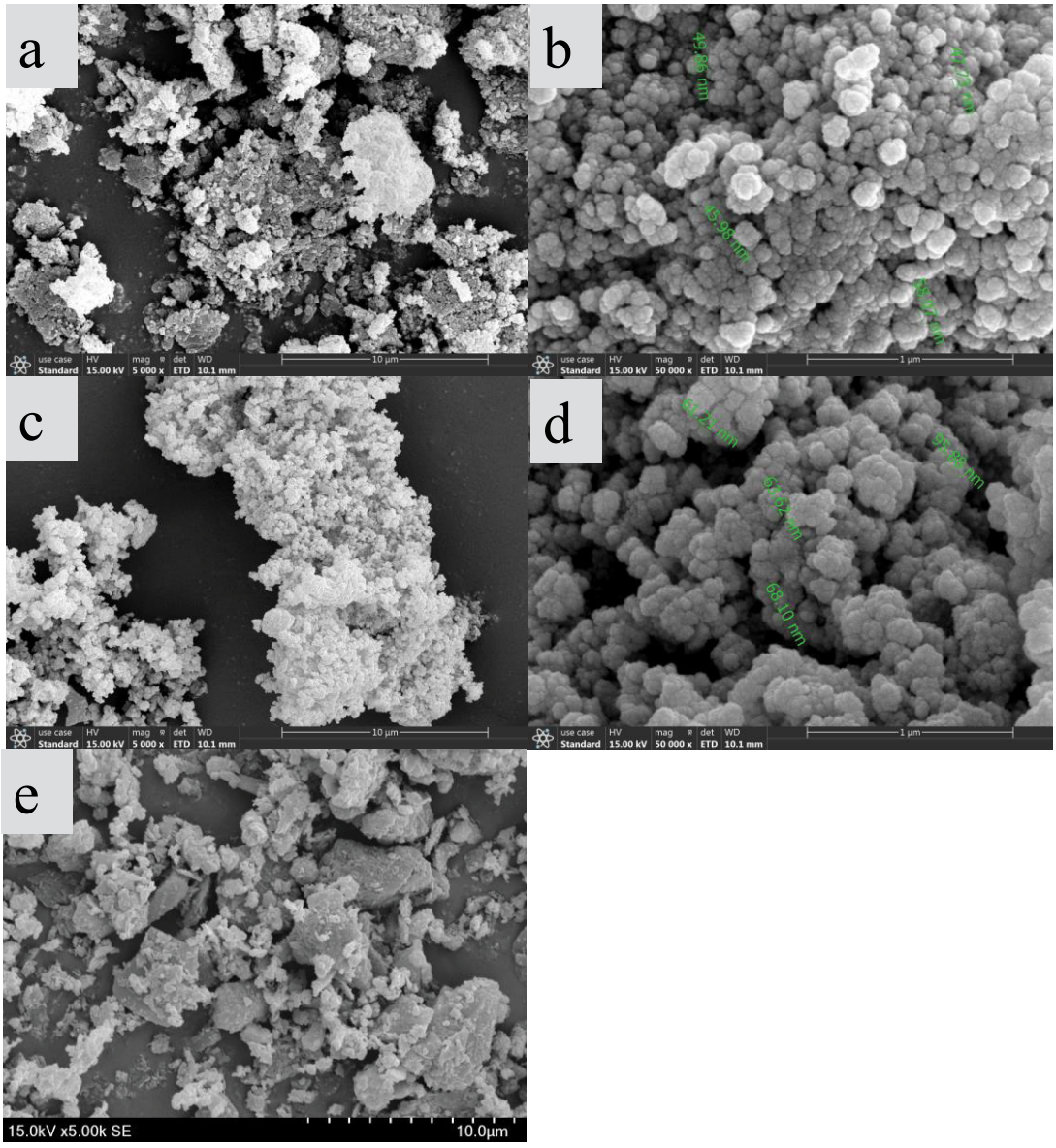

Fig. 3. SEM images. (a) IIP@SC (×5,000), (b) IIP@SC (×50,000), (c) NIP@SC (×5,000), (d) NIP@SC (×50,000), and (e) SC (×5,000).

The Cr(III) ions could be almost completely eluted by 4.0 mol/L of HNO_3 (Fig. 4b).

3.2. Adsorption performance

3.2.1. Effect of adsorbent dosage and the initial pH

The effects of adsorbent dosage toward Cr(III) ions were performed at pH 6.0 and 25°C for 120 min by varying the adsorbent dosage from 5 mg to 80 mg (Fig. 5). The sorption efficiency increases quickly with the increase of IIP@SC dose, and reaches equilibrium at 50 mg. The effects of the initial pH on the adsorption of Cr(III) ions by IIP@SC were performed in 50 mL polyethylene tubes containing 30 mL of 100 mg/L Cr(III) ions solutions with 30 mg of adsorbent at 25°C for 120 min by varying the initial pH of the solution from 2.0 to 6.0 (Fig. 6a). The results showed that the adsorption capacity of IIP@SC is higher than NIP@SC at the same initial pH. The adsorption capacity of IIP@SC increased from 7.82 to 65.57 mg/g with the increase of solution pH from 2.0 to 6.0, and the maximum adsorption capacity of Cr(III) ions for both IIP@SC and NIP@SC was at pH 6.0. Fig. 6b shows that the point of zero charge for NIP@SC and IIP@SC is at about 1.8 and 3.0, respectively, indicating that the negatively-charged surface of both adsorbents is above 3.0. Different ionic species of Cr(III) will be existed in aqueous solutions while the pH value shifting [29]. With the increase of pH, Cr(III) ions exist in the forms of more positive charges, such as Cr^{3+}, $Cr(OH)^{2+}$, $Cr_3(OH)_4^{5+}$, $Cr(OH)^{2+}$, $Cr(OH)^{2+}$ and $Cr_3(OH)_4^{5+}$, therefore, the negatively-charged IIP@SC and NIP@SC are more favorable to combine with the positively charged Cr(III) ions in solution [30]. Furthermore, the positive Cr(III) ions are more likely combined with carboxyl groups on the adsorbents due

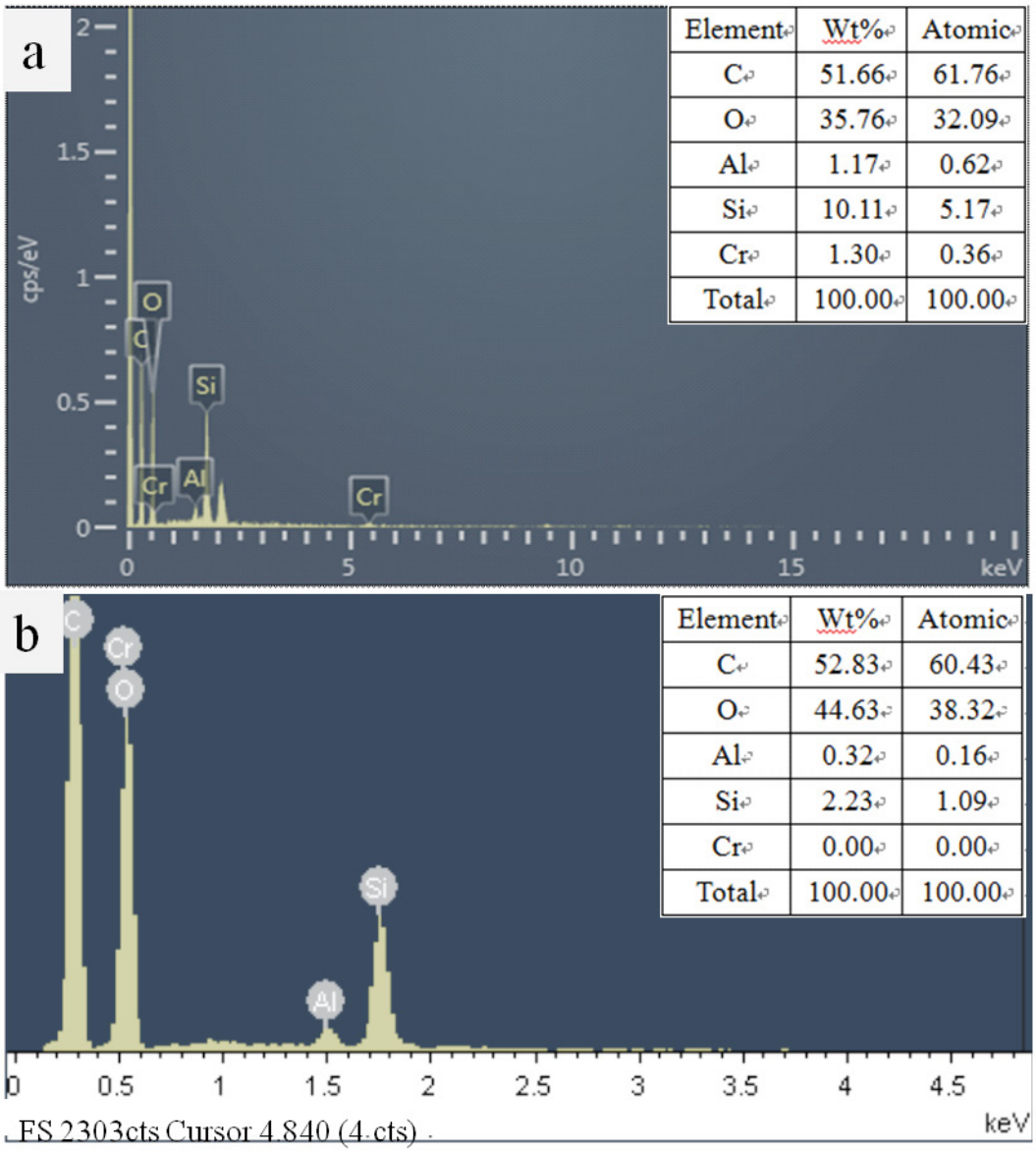

Fig. 4. Energy-dispersive X-ray spectroscopy images. (a) Cr(III)-IIP@SC and (b) IIP@SC.

to the electrostatic attraction. Moreover, a lower adsorption efficiencies of Cr(III) ion at a lower pH values might due to the presence of protons (H^+), which can compete with Cr(III) ions for occupying with the carboxyl groups [31]. While the pH value is over 6.5, $Cr(OH)_3$ precipitation appears.

3.2.2. Adsorption kinetics

The effect of the contact time on IIP@SC adsorbing of Cr(III) ions was investigated by varying the contact time from 5 to 200 min. All experiments were performed at pH 6.0 and 25°C with 30 mg of adsorbent (Fig. 7). It showed that the adsorption reached the equilibrium within 30 min and the maximum adsorption capacity was 62.83 mg/g. It also can be seen that the adsorption amount of IIP@SC was higher than that of NIP@SC, revealing that IIP@SC h ad a stronger affinity to Cr(III) ions than NIP@SC.

To investigate the mechanism of adsorption kinetics, the pseudo-first-order [Eq. (6)] and the pseudo-second-order [Eq. (7)] kinetic models are applied to fit the experimental data [32].

$$\ln\left(q_e - q_t\right) = \ln q_e - k_1 t \tag{6}$$

$$\frac{t}{q_t} = \frac{1}{k_2 q_e^2} + \frac{t}{q_e} \tag{7}$$

where q_e (mg/g) and q_t (mg/g) are the adsorption capacities at equilibrium and at an arbitrary time t (h), respectively; k_1 (1/min) and k_2 (mg/g min) are the adsorption rate constants related to pseudo-first-order equation and pseudo-second-order equation, respectively. The fitting curves are shown in Fig. S2 and the kinetic parameters are listed in Table 1. The adsorption data fitted well with the

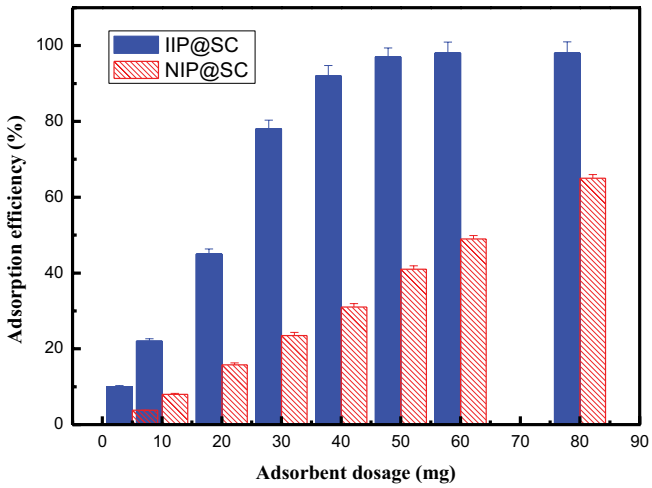

Fig. 5. Effect of adsorbent dosage on the adsorption (Cr(III) ion concentration = 100 mg/L, V = 30 mL, t = 120 min, T = 25°C).

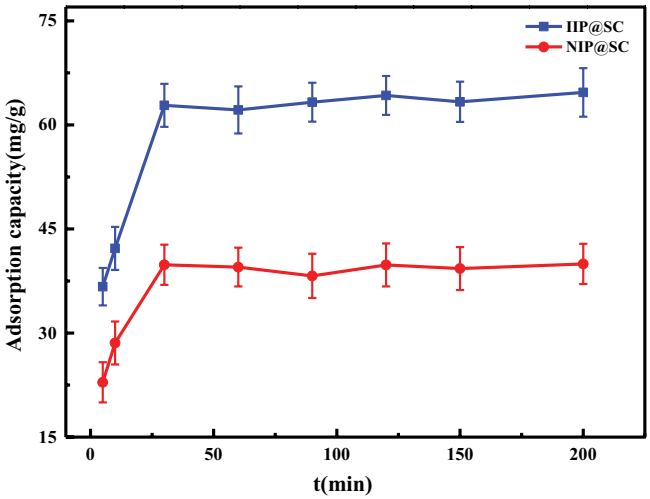

Fig. 7. Effect of contact time on adsorption. (Cr(III) ion concentration = 100 mg/L, pH = 6.0, T = 25°C).

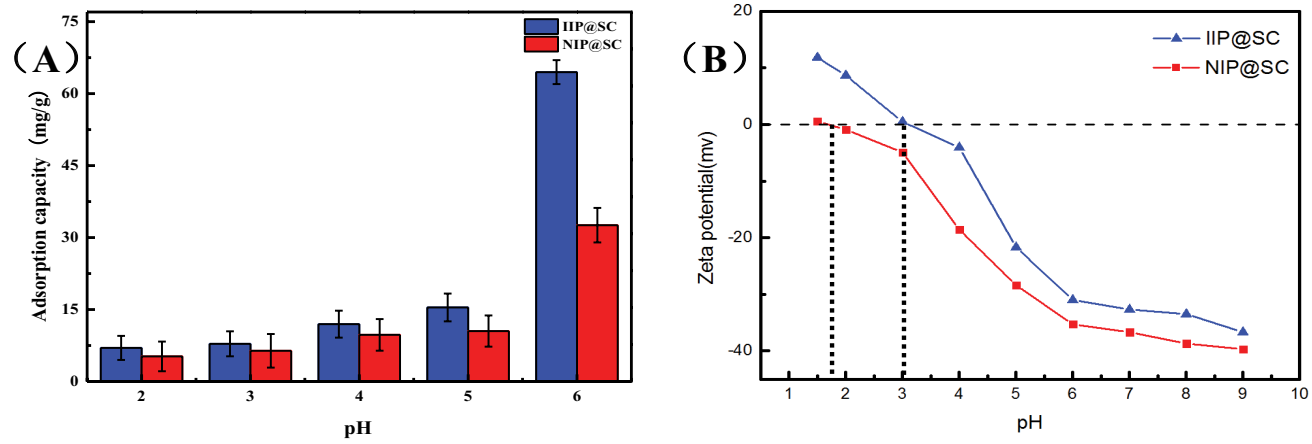

Fig. 6. (A) Effect of the initial of pH on adsorption. (Cr(III) ion concentration = 100 mg/L, t = 120 min, T = 25°C). (B) Zeta potentials of IIP@SC and NIP@SC at variant pH solutions.

Table 1
Kinetic parameters

Sample	Pseudo-first-order			Pseudo-second-order		
	q_e (mg/g)	k_1 (min^{-1})	R^2	q_e (mg/g)	k_2 (mg/g min)	R^2
IIP@SC	83.93 ± 1.18	0.17 ± 0.02	0.9611	75.82 ± 0.75	(1.31 ± 0.15) × 10^{-2}	0.9797
NIP@SC	56.83 ± 2.52	0.19 ± 0.02	0.9753	46.99 ± 0.82	(2.13 ± 0.22) × 10^{-2}	0.9960

pseudo-second-order model, with the correlation coefficient R^2 of 0.9797. The results suggest that the adsorption of Cr(III) ions on IIP@SC is mainly a chemical coordination process.

3.2.3. Adsorption isotherm

The effect of the initial concentration of Cr(III) ions was investigated by varying the concentration from 20 to 600 mg/L. All experiments were performed at pH 6.0 and 25°C for 30 min with 30 mg of adsorbent (Fig. 8). The adsorption capacity increased fast with the enhancement of concentrations of Cr(III) ions and it enhanced slowly when the concentration reached 200 mg/L. This may due to the higher ion concentration, the greater the probability of the active site being occupied. It is worth noting that the adsorption capacity of IIP@SC was much higher than that of NIP@SC, indicating more binding sites on IIP@SC.

The isothermal adsorption data were evaluated with the Langmuir [Eq. (8)] and Freundlich [Eq. (9)] equations [33,34]. The fitting results are shown in Fig. S3 and Table 2.

$$\frac{C_e}{q_e} = \frac{C_e}{q_m} + \frac{1}{K_L q_m} \tag{8}$$

$$\ln q_e = \ln K_F + \frac{\ln C_e}{n} \tag{9}$$

where C_e (mg/g) is the equilibrium concentration of Cr(III) ions, q_m (mg/g) is the maximum adsorption quantity, K_L (L/mg) is the Langmuir constant. K_F (mg/g) is a constant related to the adsorption capacity of the adsorbent and $1/n$ is a parameter indicating sorption intensity.

It shows that the experimental data of both adsorbents are fitted well with Langmuir isotherm model, with the correlation coefficient (R^2) at 0.9919 (IIP@SC) and 0.9936 (NIP@SC), respectively. Meanwhile, q_m of IIP@SC calculated by the Langmuir isotherm equation was 157.98 mg/g, which was more similar to the experimental value (137.82 mg/g). Moreover, the Langmuir adsorption capacity of IIP@SC (157.98 mg/g) was much higher than that of NIP@SC (102.14 mg/g). The results illustrate that the adsorption of Cr(III) ions by IIP@SC was a monolayer uniform adsorption mode and the ion imprinting process can significantly increase the adsorption capacity [35].

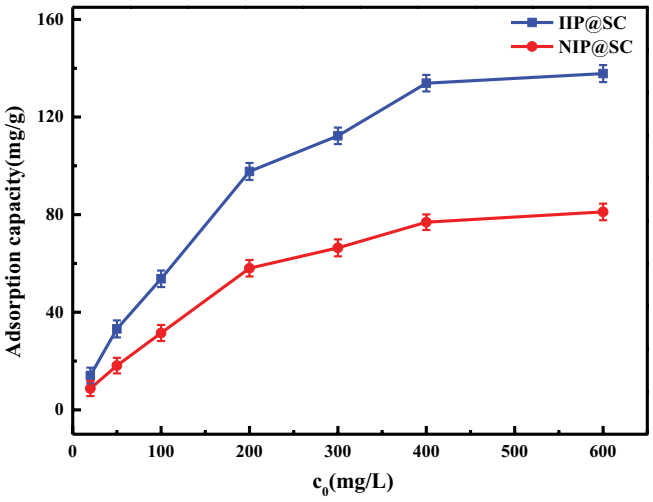

Fig. 8. Effect of the initial concentration of Cr(III) ions on adsorption. (pH = 6.0, t = 30 min, T = 25°C).

3.3. Adsorption selectivity

The adsorption selectivity of IIP@SC to Cr(III) ions were investigated by using 30 mg of the adsorbent with 30 mL of the solution containing 100 mg/L of Cr(III) ions and coexisting ions at pH 6.0 and 25°C for 120 min. The relative selectivity coefficient K' is an indicator to the selectivity performance for ion imprinting. The adsorption results and the selectivity parameters were listed in Table 3. It is showed that the adsorption capacity of Cr(III) ions on IIP@SC is obviously higher than other ions, such as Cr(VI) and Pb(II). It implies that the specific imprinted cavities on IIP@SC particle plays an important role in adsorption of Cr(III) ions when competing with other ions. It can

Table 2
Parameters of the Langmuir and Freundlich models

Sample	q_m (mg/g)	Langmuir			Freundlich		
		q_m (mg/g)	K_L (L/mg)	R^2	K_F (mg/g)	$1/n$	R^2
IIP@SC	137.82 ± 1.21	157.98 ± 1.44	(1.50 ± 0.06) × 10^{-2}	0.9919	7.24 ± 0.78	0.51 ± 0.02	0.9681
NIP@SC	81.82 ± 0.90	102.14 ± 1.08	(7.88 ± 0.25) × 10^{-3}	0.9936	2.42 ± 0.47	0.59 ± 0.01	0.9716

Table 3
K_d, K, K' parameters for IIP@SC for competing adsorption

	IIP@SC			NIP@SC			
	q_e (mg/g)	K_d (L/g)	K	q_e (mg/g)	K_d (L/g)	K	K'
Cr(III)/Cr(VI)	62.72 ± 0.66	0.50 ± 0.04	7.45 ± 0.15	24.55 ± 1.20	0.15 ± 0.04	1.51 ± 0.08	4.95 ± 0.16
	3.12 ± 0.24	(6.72 ± 0.48) × 10^{-2}		4.50 ± 0.39	(9.97 ± 0.65) × 10^{-2}		
Cr(III)/Pb(II)	48.31 ± 1.06	0.85 ± 0.07	3.76 ± 0.08	12.20 ± 0.42	0.13 ± 0.01	0.66 ± 0.05	5.69 ± 0.28
	16.58 ± 0.19	0.23 ± 0.02		14.92 ± 0.61	0.20 ± 0.01		

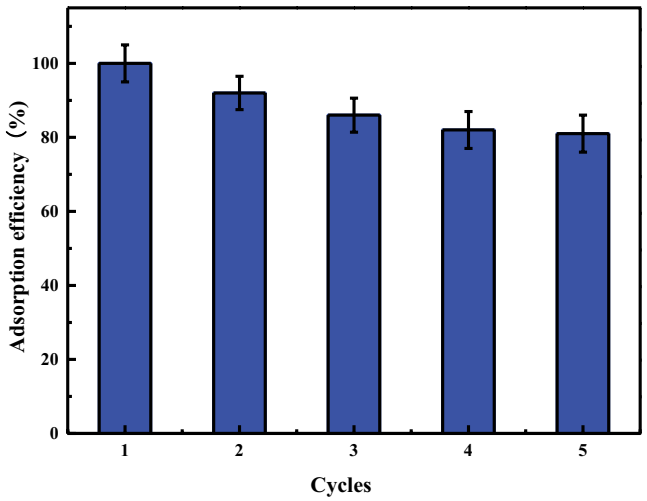

Fig. 9. Reusability of IIP@SC for Cr(III) ions recovery. (Adsorption conditions: Cr(III) ion concentration = 100 mg/L, pH = 6.0, T = 25°C; desorption conditions: 4.0 mol/L HNO_3, V/m = 5 mL/mg, t = 120 min, T = 25°C).

be seen that the values of K' are 4.95 and 5.69 for Cr(III)/Cr(VI) and Cr(III)/Pb(II), respectively. All the values of K' are much higher than 3, suggesting that IIP@SC exhibits an excellent adsorption selectivity to Cr(III) ions [36].

3.4. Desorption and reusability study

IIP@SC showed poor adsorption performance for Cr(III) ions at a lower pH range, implying that the adsorbed Cr(III) ions might be desorbed by an acid medium. In this study, the desorption of Cr(III) ions from IIP@SC was conducted with 4.0 mol/L HNO_3 solution. The degree of desorption was found to be 98.6%. The reusability of the desorbed IIP@SC was evaluated over five cycles of consecutive adsorption–desorption process (Fig. 9). It was seen that the adsorption capacity of IIP@SC was 64.56 mg/g for the first time, remained 81% (51.20 mg/g) after five desorption–adsorption process, indicating that IIP@SC has excellent regeneration property and adsorption stability towards Cr(III) ions.

4. Conclusions

In summary, we combined surface ionic imprinting technology with the porous silica clay to prepare IIP@SC with carboxyl groups for selective removal of Cr(III) ions from aqueous solution. IIP@SC showed good adsorption capacity for Cr(III) when the solution pH was at 6.0 and the adsorption temperature was 25°C. The adsorption processes followed the Langmuir model and the pseudo-second-order model. The thermodynamic study indicated that the adsorption process was exothermic and spontaneous. The prepared IIP@SC showed excellent adsorption selectivity of Cr(III) ions in solutions with co-existing ions.

Acknowledgements

This research was funded by the Open Research Fund Program of Key Laboratory of Cosmetic, China National Light Industry, Beijing Technology and Business University, (grant number: KLC-2021-YB06).

Competing interests

The authors declare no competing interest.

References

[1] E. Erdem, N. Karapinar, R. Donat, The removal of heavy metal cations by natural zeolites, J. Colloid Interface Sci., 280 (2004) 309–314.
[2] N. Adimalla, Assessment and mechanism of fluoride enrichment in groundwater from the hard rock terrain: a multivariate statistical approach, Geochem. Int., 58 (2020) 456–471.
[3] M. Malovanyy, O. Palamarchuk, I. Trach, H. Petruk, H. Sakalova, K. Soloviy, T. Vasylinych, I. Tymchuk, N. Vronska, Adsorption extraction of chromium ions (III) with the help of bentonite clays, J. Ecol. Eng., 21 (2020) 178–185.
[4] Y. Liu, X. Meng, J. Han, Z. Liu, M. Meng, Y. Wang, R. Chen, S. Tian, Speciation, adsorption and determination of chromium(III) and chromium(VI) on a mesoporous surface imprinted polymer adsorbent by combining inductively coupled plasma atomic emission spectrometry and UV spectrophotometry, J. Sep. Sci., 36 (2013) 3949–3957.
[5] B. Reyes-Romero, A.N. Gutiérrez-López, R. Hernández-Altamirano, V.Y. Mena-Cervantes, E. Ruiz-Baca, E.E. Neri-Torres, I. Chairez, S.M. García-Solares, J. Vazquez-Arenas, Removal of concentrated Cr(III) from real tannery wastewater using abiotic and anaerobic processes with native microbial consortia, J. Environ. Chem. Eng., 9 (2020) 104626, doi: 10.1016/j.jece.2020.104626.
[6] B. Wang, Y.-C. Sun, R.-C. Sun, Fractionational and structural characterization of lignin and its modification as biosorbents for efficient removal of chromium from wastewater: a review, J. Leather Sci. Eng., 1 (2019) 5, doi: 10.1186/s42825-019-0003-y.
[7] J. Pan, J. Jiang, R. Xu, Adsorption of Cr(III) from acidic solutions by crop straw derived biochars, J. Environ. Sci., 25 (2013) 1957–1965.
[8] E. Villagrasa, C. Palet, I. López-Gómez, D. Gutiérrez, I. Esteve, A. Sánchez-Chardi, A. Solé, Cellular strategies against metal

exposure and metal localization patterns linked to phosphorus pathways in *Ochrobactrum anthropi* DE2010, J. Hazard. Mater., 402 (2020) 123808, doi: 10.1016/j.jhazmat.2020.123808.
[9] Y. Chen, Q. Chen, H. Zhao, J. Dang, R. Jin, W. Zhao, Y. Li, Wheat straws and corn straws as adsorbents for the removal of Cr(VI) and Cr(III) from aqueous solution: kinetics, isotherm, and mechanism, ACS Omega, 5 (2020) 6003–6009.
[10] Z. Yin, B. Chen, M. Chen, S. Hu, H. Cheng, Recovery of chromium(III) ions from aqueous solution by carboxylate functionalized wool fibres, J. Soc. Leather Technol. Chem., 99 (2015) 101–106.
[11] O. Njoya, S. Zhao, Y. Qu, J. Shen, B. Wang, H. Shi, Z. Chen, Performance and potential mechanism of Cr(VI) reduction and subsequent Cr(III) precipitation using sodium borohydride driven by oxalate, J. Environ. Manage., 275 (2020) 111165, doi: 10.1016/j.jenvman.2020.111165.
[12] B. Jiang, Q. Niu, C. Li, N. Oturan, M.A. Oturan, Outstanding performance of electro-Fenton process for efficient decontamination of Cr(III) complexes via alkaline precipitation with no accumulation of Cr(VI): important roles of iron species, Appl. Catal., B, 272 (2020) 119002, doi: 10.1016/j.apcatb.2020.119002.
[13] S. Mustapha, J.O. Tijani, M.M. Ndamitso, S.A. Abdulkareem, D.T. Shuaib, A.K. Mohammed, A. Sumaila, The role of kaolin and kaolin/ZnO nanoadsorbents in adsorption studies for tannery wastewater treatment, Sci. Rep., 10 (2020) 13068, doi: 10.1038/s41598-020-69808-z.
[14] S. Kaushal, N. Kaur, M. Kaur, P.P. Singh, Dual-responsive pectin/graphene oxide (Pc/GO) nano-composite as an efficient adsorbent for Cr(III) ions and photocatalyst for degradation of organic dyes in waste water, J. Photochem. Photobiol., A, 403 (2020) 112841, doi: 10.1016/j.jphotochem.2020.112841.
[15] J. Li, H. Cheng. Ion-imprinted modified molecular sieves show the efficient selective adsorption of chromium(VI) from aqueous solutions, RSC Adv., 10 (2020) 43425–43431.
[16] J. Zeng, J. Zeng, H. Zhou, G. Liu, Z. Yuan, J. Jian, Ion-imprinted silica gel and its dynamic membrane for nickel ion removal from wastewaters, Front. Chem. Sci. Eng., 14 (2020) 1018–1028.
[17] T. Fang, X. Yang, L. Zhang, J. Gong, Ultrasensitive photoelectrochemical determination of chromium(VI) in water samples by ion-imprinted/formate anion-incorporated graphitic carbon nitride nanostructured hybrid, J. Hazard. Mater., 312 (2016) 106–113.
[18] M. Jamshidi, M. Ghaedi, K. Dashtian, S. Hajati, New ion-imprinted polymer-functionalized mesoporous SBA-15 for selective separation and preconcentration of Cr(III) ions: modeling and optimization, RSC Adv., 5 (2015) 105789–105799.
[19] Q.-y. Zhu, L.-y. Zhao, D. Sheng, Y.-j. Chen, X. Hu, H.-z. Lian, L. Mao, X.-b. Cui, Speciation analysis of chromium by carboxylic group functionalized mesoporous silica with inductively coupled plasma mass spectrometry, Talanta, 195 (2019) 173–180.
[20] M. Gutiérrez-Valtierra, C. Salazar-Hernández, J.M. Mendoza-Miranda, E. Elorza-Rodríguez, P. Alquiza, M. Caudillo-González, M. Salazar, Cr(III) removal from tannery effluents using silica obtained from rice husk and modified silica, Desal. Water Treat., 158 (2019) 152–163.
[21] Z. Zhao, X. Zhang, H. Zhou, G. Liu, M. Kong, G. Wang, Microwave-assisted synthesis of magnetic Fe_3O_4-mesoporous magnesium silicate core-shell composites for the removal of heavy metal ions, Microporous Mesoporous Mater., 242 (2017) 50–58.
[22] W. Kuchen, J. Schram, Metal-ion-selective exchange resins by matrix imprint with methacrylates, Angew. Chem. Int. Ed., 27 (1988) 1695–1697.
[23] N. Ozkantar, M. Soylak, M. Tuzen, Ultrasonic-assisted supramolecular solvent liquid-liquid microextraction for inorganic chromium speciation in water samples and determination by UV-Vis spectrophotometry, At. Spectrosc., 41 (2020) 43–50.
[24] H. Vergara-Castañeda, A.R. Hernandez-Martinez, M. Estevez, S. Mendoza, G. Luna-Barcenas, H. Pool, Quercetin conjugated silica particles as novel biofunctional hybrid materials for biological applications, J. Colloid Interface Sci., 466 (2016) 44–55.
[25] Z. Ren, D. Kong, K. Wang, W. Zhang, Preparation and adsorption characteristics of an imprinted polymer for selective removal of Cr(VI) ions from aqueous solutions, J. Mater. Chem. A, 2 (2014) 17952–17961.
[26] S. Selmani, A. Sdiri, S. Bouaziz, E. Joussein, S. Rossignol, Effects of metakaolin addition on geopolymer prepared from natural kaolinitic clay, Appl. Clay Sci., 146 (2017) 457–467.
[27] H. Jadli, J. Brahmi, A. Chrouda, A. Jbara, S.G. Almalki, G. Osman, K. Slimi, CO_2 adsorption performance of amine clay adsorbent, Appl. Phys., A, 127 (2021) 54, doi: 10.1007/s00339-020-04142-9.
[28] M. Ghanei-Motlagh, M.A. Taher, A. Heydari, R. Ghanei-Motlagh, V.K. Gupta, A novel voltammetric sensor for sensitive detection of mercury(II) ions using glassy carbon electrode modified with graphene-based ion-imprinted polymer, Mater. Sci. Eng., C, 63 (2016) 367–375.
[29] N.F. Fahim, B.N. Barsoum, A.E. Eid, M.S. Khalil, Removal of chromium(III) from tannery wastewater using activated carbon from sugar industrial waste, J. Hazard. Mater., 136 (2006) 303–309.
[30] D. Ma, S. Hu, Y. Li, Z. Xu, Adsorption of uranium on phosphoric acid-activated peanut shells, Sep. Sci. Technol., 55 (2020) 1623–1635.
[31] S.-T. Hsu, T.-C. Pan, Adsorption of paraquat using methacrylic acid-modified rice husk, Bioresour. Technol., 98 (2007) 3617–3621.
[32] N. Zhao, H. Huang, X. Lv, J. Li, G. Guo, Y. Liu, Removal of Cr(III) from aqueous solutions using waste kelp-derived biochar, Desal. Water Treat., 188 (2020) 223–231.
[33] M. Zhu, D. Fan, B. Liu, S. Liu, M. Fang, X. Tan, $C@K_2Ti_6O_{13}$ hierarchical nano materials: effective adsorption removal of Cr(VI), J. Inorg. Mater., 35 (2019) 309–314.
[34] Q. Liang, J. Geng, H. Luo, W. Fang, Y. Yin, Fast and selective removal of Cr(VI) from aqueous solutions by a novel magnetic Cr(VI) ion-imprinted polymer, J. Mol. Liq., 248 (2017) 767–774.
[35] Y. Andelib Aydın, N. Deveci Aksoy, Adsorption of chromium on chitosan: optimization, kinetics and thermodynamics, Chem. Eng. J., 151 (2009) 188–194.
[36] Y.A.B. Neolaka, G. Supriyanto, H.S. Kusuma, Adsorption performance of Cr(VI)-imprinted poly(4-VP-co-MMA) supported on activated Indonesia (Ende-Flores) natural zeolite structure for Cr(VI) removal from aqueous solution, J. Environ. Chem. Eng., 6 (2018) 3436–3443.

Supplementary information

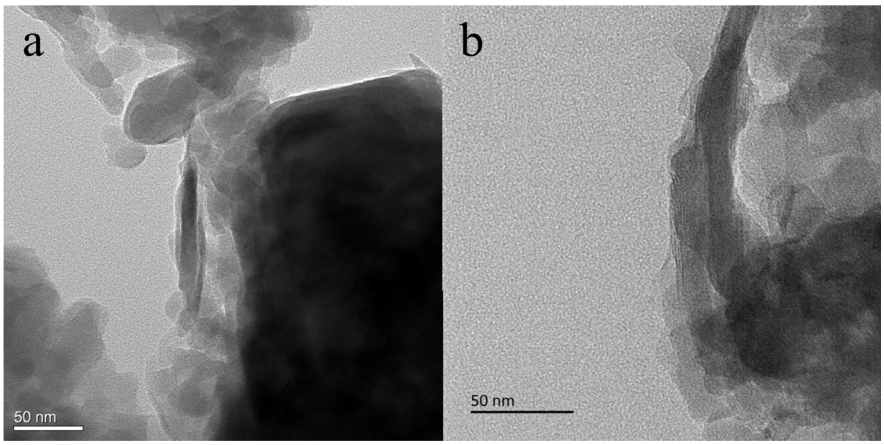

Fig. S1. TEM images. (a) Silica clay and (b) IIP@SC.

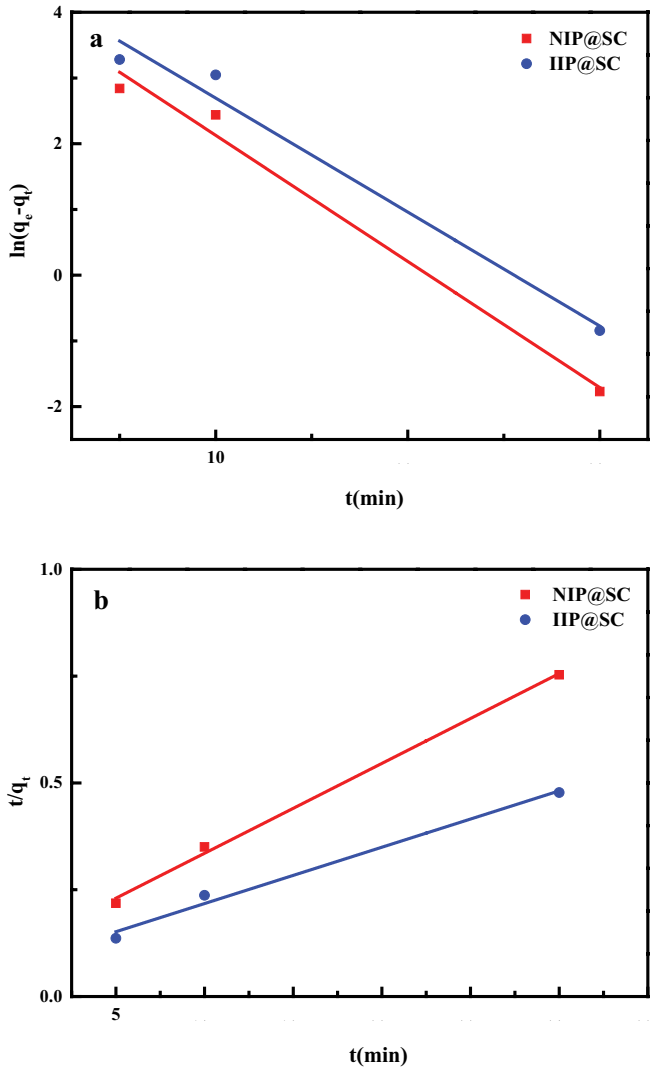

Fig. S2. (a) Pseudo-first-order and (b) pseudo-second-order model kinetic plots for Cr(III) adsorption onto IIP@SC and NIP@SC. Conditions: pH = 6.0, T = 25°C, C_0 = 100 mg/L.

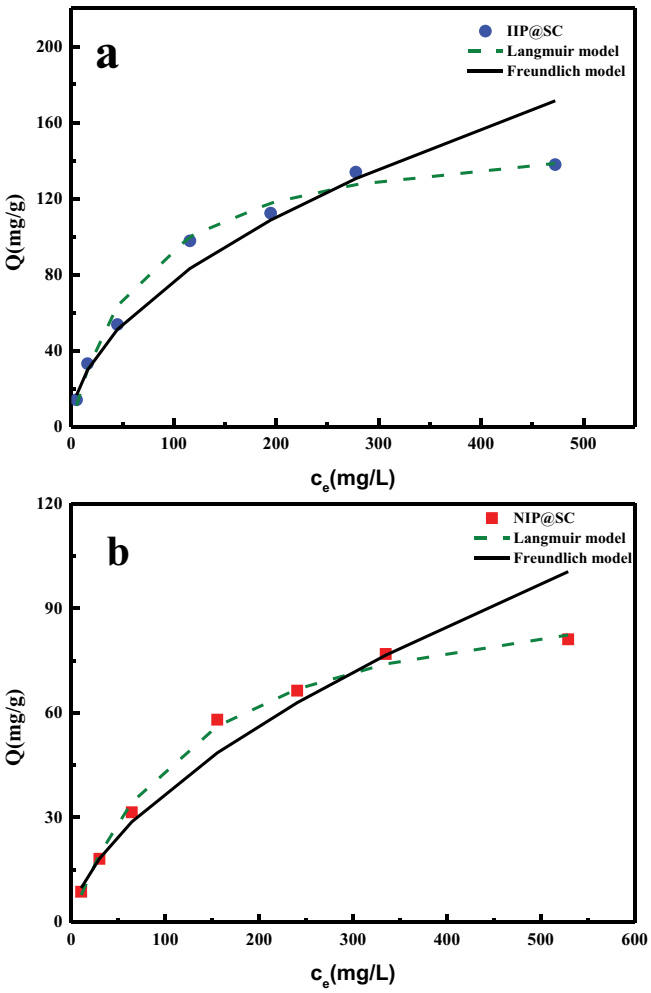

Fig. S3. Absorption isotherms: (a) IIP@SC and (b) NIP@SC. Conditions: pH = 6.0, T = 25°C, t = 30 min.